Journal of Solid State Chemistry 184 (2011) 7–11

Contents lists available at ScienceDirect

Journal of Solid State Chemistry

journal homepage: www.elsevier.com/locate/jssc

Silver delafossite nitride, $AgTaN_2$?

Akira Miura [a,b], Michael Lowe [b], Brian M. Leonard [b,1], Chinmayee V. Subban [b], Yuji Masubuchi [c], Shinichi Kikkawa [c], Richard Dronskowski [a], Richard G. Hennig [d], Héctor D. Abruña [b], Francis J. DiSalvo [b,*]

[a] Institute of Inorganic Chemistry, RWTH Aachen University, Landoltweg 1, 52074 Aachen, Germany
[b] Department of Chemistry and Chemical Biology, Baker Laboratory, Cornell University, Ithaca, New York 14853, United States
[c] Graduate School of Engineering, Hokkaido University, N13W8, Kita-ku Sapporo 060-8628, Japan
[d] Department of Materials Science and Engineering, Cornell University, Ithaca, New York 14853, United States

ARTICLE INFO

Article history:
Received 23 August 2010
Received in revised form
1 October 2010
Accepted 5 October 2010
Available online 12 November 2010

Keywords:
Nitride
Delafossite
Topotactic reaction
Exchange reaction
Soft chemistry

ABSTRACT

A new silver nitride, $AgTaN_2$, was synthesized from $NaTaN_2$ by a cation-exchange reaction, using a $AgNO_3$–NH_4NO_3 flux at 175 °C. Its crystal structure type is delafossite ($R\bar{3}m$) with hexagonal lattice parameters of $a=3.141(3)$ Å, $c=18.81(2)$ Å, in which silver is linearly coordinated to nitrogen. Energy dispersive X-ray analysis and combustion nitrogen/oxygen analysis gave a composition with atomic ratios of Ag:Ta:N:O as 1.0:1.2(1):2.1(1):0.77(4), which is somewhat Ta rich and indicates some oxide formation. The X-ray photoelectron spectroscopy analysis showed a Ta- and O-rich surface and transmission electron microscope observation exhibited aggregates of ca. 4–5 nm-sized particles on the surface, which are probably related to the composition deviation from a $AgTaN_2$. The lattice parameters of stoichiometric $AgTaN_2$ calculated by density functional theory agree with the experimental ones, but the possibility of some oxygen incorporation and/or silver deficiency is not precluded.

1. Introduction

A number of ternary and quaternary nitrides have been reported in the last three decades, together with magnetic, electronic, optical and catalytic properties [1–4]. One of the remaining challenges in this field is to synthesize nitrides, which contain bonding between precious metals and nitrogen. The existence of silver–nitrogen bonding demonstrates this challenge. For example, three silver calcium nitrides have been synthesized [5–7]. However, these ternary nitrides do not contain silver–nitrogen bonding; the nitrogen atoms are surrounded by calcium atoms. Another example is an antiperovskite silver manganese nitride, $AgMn_3N$, in which only manganese occupies the nearest neighbor positions around nitrogen [8]. These bonding characteristics are likely attributed to low bonding energies between precious metals and nitrogen. When compared with oxides, nitrides are less thermodynamically stable due to the strong triple bond in molecular nitrogen. Since even binary precious metal oxides have small free energies of formation at room temperature under atmospheric pressure [9], ternary nitrides with bonding between precious metals and nitrogen are expected to be even less thermodynamically stable. Therefore, synthesis of nitrides containing this bonding should be performed by low temperature and/or high pressure pathways.

Copper tantalum nitride ($CuTaN_2$) was synthesized by a cation-exchange reaction of sodium tantalum nitride ($NaTaN_2$) by heating with CuI at 400 °C [10]. The crystal structure is a hexagonal delafossite-type (or α-$NaFeO_2$ type) (Fig. 1). This is a layered structure, in which Cu is linearly coordinated to N and Ta is the center of a nitrogen octahedron. While this is the only reported delafossite nitride with a monovalent transition metal in linearly coordinated position, many delafossite oxides with the metals (Cu, Ag, Pd and Pt) in the same position have been synthesized [9,11,12]. In these oxides, monovalent and trivalent metals occupy the positions of Cu and Ta in $CuTaN_2$, respectively. A number of these delafossite oxides have potential applications, such as thermoelectronic materials [13], p-type transparent electrodes [14], electrocatalysts [15] and photocatalysts [16,17], which motivated us to explore structurally related nitrides.

Here, we report a new ternary delafossite nitride, $AgTaN_2$. To our knowledge, this is the first ternary nitride in which silver atoms have nearest neighbor nitrogen atoms. This nitride is synthesized by a cation-exchange reaction using a nitrate flux, which has been commonly utilized for the synthesis of oxides [18], but not for nitrides.

2. Experimental procedure

$AgTaN_2$ was synthesized in three steps: ammonolysis of $TaCl_5$ to synthesize Ta_3N_5, followed by the reaction of Ta_3N_5 with Na, and

* Corresponding author. Fax: +1 607 255 4137.
E-mail address: fjd3@cornell.edu (F.J. DiSalvo).
[1] Current address: Brian M. Leonard, Department of Chemistry, University of Wyoming, 1000 E. University Avenue, Laramie, Wyoming 82071, United States.

0022-4596/$ - see front matter © 2010 Elsevier Inc. All rights reserved.
doi:10.1016/j.jssc.2010.10.009

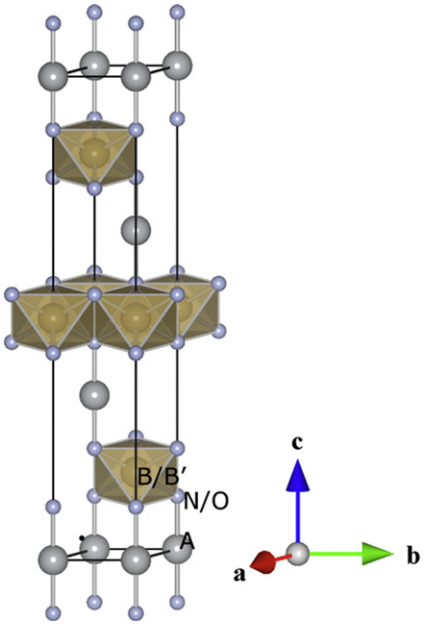

Fig. 1. Crystal structure of delafossite ABN_2 or $AB'O_2$, in which A, B, B' are monovalent, pentagonal and trivalent cations, respectively. *A* cations are described in large spheres, and B/B' cations are located in octahedra of anions (either N or O) shown in small spheres. This scheme is drawn by VESTA [29].

finally an exchange reaction to prepare $AgTaN_2$ from $NaTaN_2$. All the reagents were handled in an Ar-filled glove box for the synthesis of Ta_3N_5 and $NaTaN_2$, and an exchange reaction was performed in air. Dark red Ta_3N_5 powder was obtained by heating $TaCl_5$ (Alfa Chemicals 99.99%) at 700 °C in an ammonia flow for 1 h [10]. Yellow $NaTaN_2$ powder was produced by heating Ta_3N_5 and Na metal (Aldrich 99%) at 500 °C in an alumina boat under an ammonia flow, and heated the products again at 700 °C under an ammonia flow after removal of $NaNH_2$ in the glove box [10]. In the third step, $NaTaN_2$ was mixed with $AgNO_3$ (Mallinckrodt 99.9%) and NH_4NO_3 (Mallinckrodt Analytical Grade) in a molar ratio of 1:1:4 in air. This mixture was heated at 175 °C for 16 h, and washed with distilled water to remove water-soluble byproducts or remaining reactants ($AgNO_3$, NaCl, NH_4NO_3). Further washing with a 1 M ammonia aqueous solution was performed to remove AgCl contaminants, which are presumably formed by the reaction of $AgNO_3$ with Cl coming from trace amounts of $TaCl_5$, from unidentified tantalum nitride chlorides or from NH_4Cl contamination (byproduct of Ta_3N_5).

Powder X-ray diffraction (pXRD; Rigaku Ultima IV; Cu $K\alpha$ radiation) with Bragg Brentano Geometry over a scan range 10–120° was used for structural characterization. Lattice parameters were calculated by peaks indexed in the 2θ range 10–75°. The Ag/Ta ratio was semiquantitatively determined by energy dispersive X-ray analysis (EDX: LEO-1550 field emission SEM) at seven different positions of the powder smeared on an Al plate. The ratio was also determined by the peak ratio of pXRD peaks of $AgTaO_3$–$Ag_2Ta_4O_{11}$ after an oxidation of the nitride sample by heating at 1000 °C for 30 min in air. A calibration line of the peak ratio was obtained by heating the mixture of Ag_2CO_3 (Mallinckrodt analytical grade) and Ta_2O_5 powders (Sigma Aldrich 99%) with various ratios by a conventional ceramics method. The oxygen and nitrogen contents were measured by the combustion method using a Horiba elemental analyzer (EMGA, EF-620 W). Images were taken with a transmission electron microscope (TECNAI T-12 TEM) equipped with selected area electron diffraction (SAED). The samples were prepared by suspending the particles in 5 ml of degassed isopropyl alcohol and sonicating using a 3150 Bransonic ultrasonic cleaner. This solution was then dropped onto a carbon coated copper grid. Surface characterization of the sample on carbon tape was carried out by X-ray photoelectron spectroscopy (XPS; Surface Science Instrument SSX-100). No Ar etching was performed in order to avoid the possible decomposition of Ag and Ta compounds [19–21]. Signals of Ag3d (364–379 eV), Ta4d(220–250 eV), N1s(390–414 eV) and O1s(523–537 eV) were employed to determine atomic ratios. Optical absorption was measured with a J&M Tidas (Zeiss Axioplan 2) Heraeus spectrometer.

The theoretical crystal structures of $AgTaN_2$ and $CuTaN_2$ were calculated by density functional theory (DFT), as implemented in the Vienna Ab-initio Simulation Package (VASP) v. 4.6.31[22]. The core electronic states are described by projector augmented-wave (PAW) potentials [23]. The PBE generalized-gradient approximation was used for the exchange-correlation functional [24]. The energy cutoff for plane waves was 400 eV, and the Brillouin zone integration was performed using the tetrahedron method with Blöchl corrections on an automatically generated Monkhorst–Pack grid of $22 \times 22 \times 3$ k points. The experimentally obtained lattice parameters and the relative atomic position of nitrogen reported in $CuTaN_2$ were given as initial data and these values were optimized using a conjugate gradient algorithm without consideration of the initial symmetry. The crystal structure of hypothetical $AgTaO_2$ was also calculated by a similar procedure for $AgTaN_2$, but nitrogen was replaced by oxygen.

3. Results and discussion

$NaTaN_2$ was a yellow, highly crystalline and single-phase product as determined by the X-ray diffraction (maximum crystalline impurities below 5 wt%). A dark red powder was obtained after the exchanging Na^+ for Ag^+ using a $AgNO_3$–NH_4NO_3 flux at 175 °C. The color and pXRD pattern of the powder did not change after six months in air. The synthesized $AgTaN_2$ powder was stable under exposure to the laboratory X-ray source, but not to the synchrotron beam: the sample color darkened noticeably during the course of measurement. No changes have been observed by an electron beam irradiation during SEM and TEM observations.

Fig. 2 shows the powder X-ray diffraction pattern of the dark red powder after washing. The diffraction peaks are indexed on a hexagonal lattice similar to $CuTaN_2$, together with minor impurity peaks from silver metal. The presence of silver metal is not surprising, since this is often observed as an impurity in silver delafossite oxides [18]. The measured lattice parameters are $a=3.141(3)$ Å and $c=18.81(2)$ Å. The intensity ratios of the diffraction peaks are close to those calculated for a delafossite-type

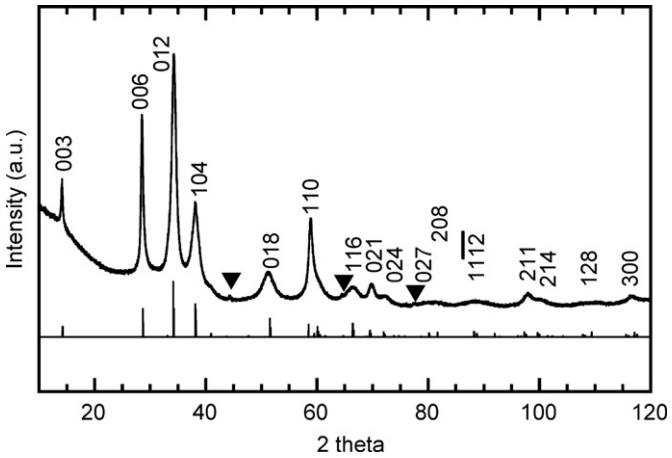

Fig. 2. pXRD patterns of $AgTaN_2$ synthesized by heating $NaTaN_2$ with $AgNO_3$/NH_4NO_3 at 175 °C. Markers indicate silver metal peaks. Pattern shown below is a simulated one for $AgTaN_2$.

structure for $AgTaN_2$, of which the nitrogen position was determined by the computational calculation described below. Thus, this demonstrates that the $AgTaN_2$ delafossite-type phase can be obtained by a cation-exchange reaction. The peak broadening is observed for the hkl reflections, where at least h or k and l are non-zero; for example, 012, 104, 018 peaks are much broader than 003, 006, 110 peaks. This can be attributed to a stacking disorder along the *c*-axis [25]. We confirmed this broadening feature is not predominantly caused by the presence of Cu $K\alpha_2$ radiation, since little change is observed in the pXRD pattern obtained from a pure Cu $K\alpha_1$ X-ray source. Rietveld analysis was not performed because of the low crystallinity.

EDX did not show a sodium signal at ca. 1 eV, indicating a complete exchange reaction (Fig. 3). The Ag/Ta ratio semiquantitatively measured by EDX was 0.82(7). After oxidation of the sample at 1000 °C in air, pXRD exhibited diffraction peaks from both $AgTaO_3$ and $Ag_2Ta_4O_{11}$. The Ag/Ta ratio determined by the peak ratio of $AgTaO_3$ and $Ag_2Ta_4O_{11}$ agrees with EDX results (0.80(5)). The amount of nitrogen determined by the combustion analysis was 7.2 wt%, less than the calculated value of 8.8 wt% for $AgTaN_2$. A 3.6 wt% of oxygen was also detected. An overall composition ratio of Ag:Ta:N:O in the product is 1.0:1.2(1):2.1(1):0.77(4), which is a somewhat Ta- and definitely O-rich composition compared to stoichiometric $AgTaN_2$.

This deviation from stoichiometric $AgTaN_2$ may be explained by Ta–O rich impurity phases that is possibly amorphous and/or very small crystalline particles. This could be a surface phase formed by reaction with the nitrate in the flux. The small amount of silver metal impurity does not account for Ta–O rich composition deviation. Surface analysis by XPS showed Ag, Ta, N, O, and C signals with minor satellite signals (Fig. 4). The C signal is very likely attributed to surface contamination, and the ratios of Ta/Ag and O/N were 2.43 and 1.03, respectively. It is noted that the O/N ratio may be underestimated by overlapping signals from Ta4p and N1s. These XPS results indicate a Ta- and O-rich surface layer forms on $AgTaN_2$. TEM images and SAED patterns (Fig. 5) show particles of 20–100 nm in size. An SAED of these particles can be indexed with $AgTaN_2$ (Fig. 5(a)). There are some spots neither identified with $AgTaN_2$ nor silver metal, implying the presence of additional crystalline phase or phases. Fig. 3(b) shows that the surfaces of these particles are covered with aggregated smaller particles (ca. 4–5 nm). We could not obtain EDX and SAED data from only these aggregated particles, because of the limited spatial resolution of the apparatus. Nonetheless, as the composition of these small particles should be close to the results by the XPS analysis, the small aggregated particles should be a Ta–O rich composition. Even if the particles are highly crystalline, due to the small size of these particles, their pXRD diffraction peaks would be very broad and likely be too weak to be seen in the pXRD pattern of $AgTaN_2$.

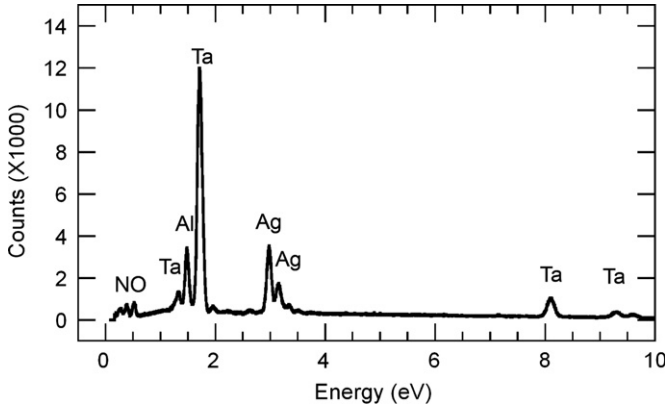

Fig. 3. Typical energy dispersive X-ray spectrum of $AgTaN_2$ powder.

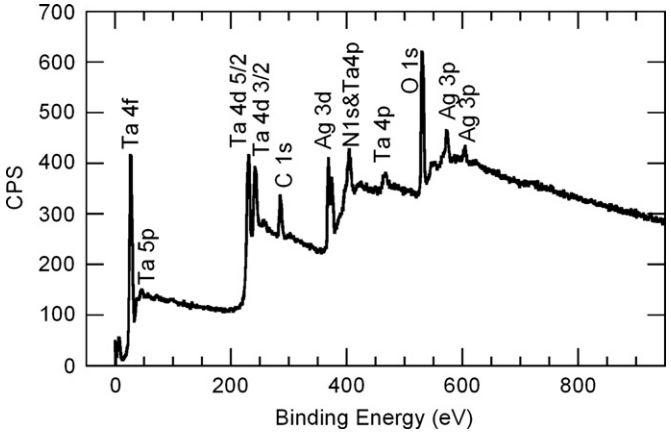

Fig. 4. X-ray photoelectron spectrum of $AgTaN_2$ powder.

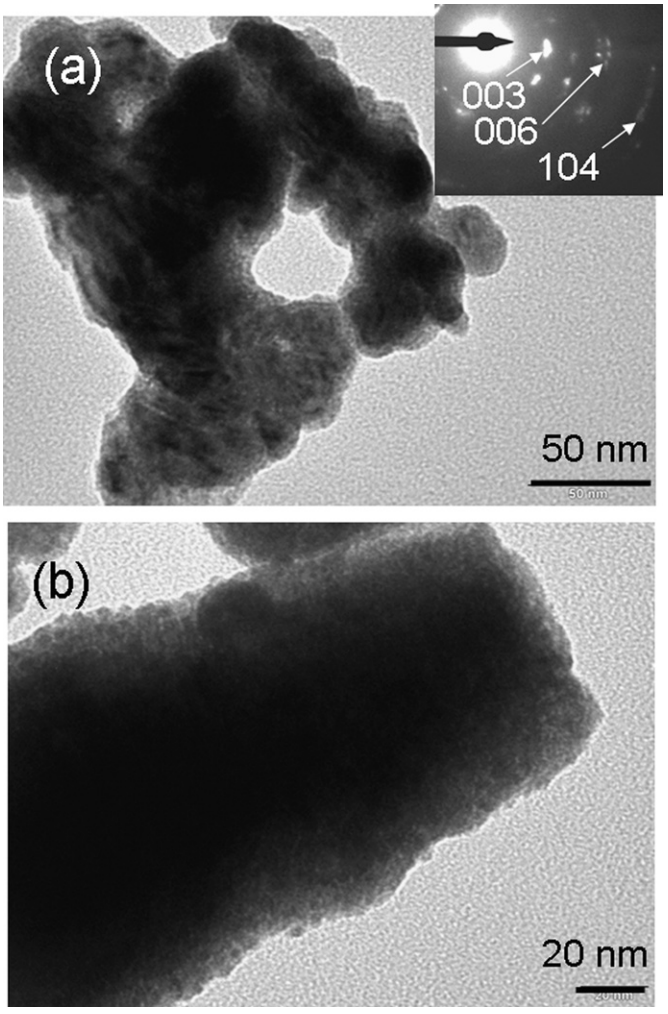

Fig. 5. (a) TEM images of $AgTaN_2$ powder with an electron diffraction pattern and (b) is a magnification of the edge of the particles.

Therefore, a Ta–O rich surface of $AgTaN_2$ is the likely reason for the measured composition deviation of that of $AgTaN_2$, though we cannot rule out the possibility of silver deficiency or some oxygen on nitrogen sites of $AgTaN_2$ itself.

Density-functional calculations were performed for stoichiometric $CuTaN_2$, $AgTaN_2$ and hypothetical $AgTaO_2$. This $AgTaN_2$ is a structure with a minimum energy hypersurface, and the formation of $AgTaN_2$

Table 1
Summary of lattice parameters: 'exp.' and 'cal.' indicate the values from XRD and DFT–GGA calculation, respectively.

Compounds	Lattice parameters (Å)		Volume (Å^3)
	a	c	
$AgTaN_2$ (exp., this work)	3.141(3)	18.81(2)	160.7
$AgTaN_2$ (cal., this work)	3.15	19.06	163.8
$AgTaO_2$ (cal., this work)	2.98	22.62	174.0
$AgFeO_2$ (exp. [9])	3.0391(2)	18.590(2)	148.7
$AgGaO_2$ (exp. [9])	2.9889(2)	18.534(2)	143.4
$CuTaN_2$ (exp. [10])	3.136(1)	17.438(5)	148.5
$CuTaN_2$ (cal., this work)	3.15	17.59	151.2
$CuFeO_2$ (exp. [9])	3.0351(2)	17.156(2)	136.9
$CuGaO_2$ (exp. [9])	2.9750(2)	17.154(2)	131.4

from Ag, Ta and N_2 elements is exothermic. The optimized lattice parameters are shown in Table 1. The lattice parameters of stoichiometric $CuTaN_2$ and $AgTaN_2$ are close to experimental values with deviation less than 1.6%. On the other hand, the lattice parameters of the hypothetical same-structured $AgTaO_2$ exhibit a 22.3% longer *c*-axis than that of experimentally obtained $AgTaN_2$. This disagreement denies the hypothetical $AgTaO_2$. These calculations show that the pXRD pattern of $AgTaN_2$ can be attributed to nearly stoichiometric $AgTaN_2$, though we cannot disprove the possibility of some oxygen incorporation or a small silver deficiency. The calculated *z* parameter of the atomic position of nitrogen in $AgTaN_2$ is 0.111; all other atomic parameters of *x*, *y* and *z* for Ag, Ta and N are special positions. As a result, calculated lengths of Ag–N and Ta–N are 2.12 and 2.11 Å, respectively. Although a small difference of lattice parameters and bonding distance is commonly observed between experimental and computational values (generally less than 3%), the calculated bonding lengths in $AgTaN_2$ are close to related experimental values. The bonding length of Ag–N is close to those of Ag–O in silver delafossite oxides (2.066–2.123 Å) [18], and the length of Ta–N is comparable with those in $NaTaN_2$ (2.123 Å) [26]. When compared with delafossite $CuTaN_2$, both the lengths of Ag–N and Ta–N are longer than those of Cu–N (2.08 Å) and Ta–N (1.99 Å) [10].

The effect of ionic radius on delafossite materials is of interest (Table 1). For delafossite ABO_2 oxides (*A* is Cu or Ag, and *B* is a trivalent metal, such as Al, Ga, In, Fe, Cr, Co, Sc, Ru), the *a*-axis linearly increases with the ion radius of the B metal and the *c*-axis mainly depends on that of the *A* metal [27]. The two delafossite nitrides seem to follow this trend though this comparison is restricted for only two examples. When the lattice parameters of $AgTaN_2$ are compared with isostructural $CuTaN_2$ (Table 1), the *a*-axis is almost the same but the *c*-axis is expanded, because of the larger ionic radius of Ag^+ (67 pm [28]) compared to Cu^+ (46 pm [28]). The lattice parameters of selected oxides are listed in Table 1 in order to discuss the difference between oxides and nitrides. We choose Fe and Ga as *B* metals for ABO_2, since the ionic radii of Fe^{3+} (64.5 pm [28]) and Ga^{3+} (62 pm [28]) are similar to that of Ta^{5+} (64 pm [28]). Within the comparisons between Cu-compounds and between Ag-compounds, the volumes of the nitrides are ca. 10% larger than those of the oxides because of larger ionic radius of N^{3-} (132 pm [28]) compared to O^{2-} (124 pm [28]). While the *a*-axis of nitrides expands about 5% from the oxides, the *c*-axis of nitrides increases only slightly by perhaps 1–2%. This indicates that the anion mainly affects the bonding in the octahedral layer, shown in Fig. 1.

The optical absorption of the nitride is shown in Fig. 6. A broad optical absorption was observed in 2–3 eV range. This broad absorption is similar to that of silver delafossite oxides [12].

Attempts to produce single-phase $AgTaN_2$ with high crystallinity have not been successful. No significant difference was observed in pXRD when we employed different reactant ratios of $NaTaN_2$:$AgNO_3$:NH_4NO_3 or heating different temperatures between

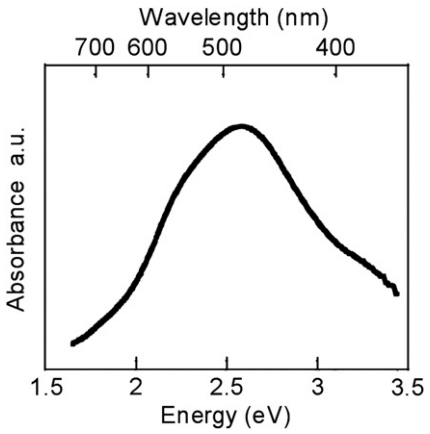

Fig. 6. Optical absorption of $AgTaN_2$ powder.

125–190 °C. The delafossite phase was not observed when $NaTaN_2$ was heated with AgI at 150–400 °C in an evacuated silica glass tube or by using a $AgNO_3$–KNO_3 flux at 330 °C. When $AgTaN_2$ was heated under an Ar flow to 500 °C, the sample color darkened and intense XRD peaks of silver metal were observed, implying the decomposition of the delafossite structure. The peaks of $AgTaN_2$ did not significantly change on heating to 400 °C, but disappeared at 500 °C.

4. Summary

An exchange reaction using a $AgNO_3/NH_4NO_3$ flux converted $NaTaN_2$ into $AgTaN_2$. The structure proposed based on pXRD is a delafossite structure (α-$NaFeO_2$ type), consisting of linear Ag–N bonding and octahedral Ta–N units. This successful exchange reaction suggests that low-temperature techniques are useful to synthesize ternary or more complex nitrides, which contain bonding between precious metals and nitrogen. A further challenge remains to obtain single-phase $AgTaN_2$ with high crystallinity. Such crystallinity is essential for further characterization, including more precise atomic positions, defect and impurity concentrations, and optical and electronic properties.

Acknowledgments

We thank Malcolm Thomas and Jonathan Shu at the Cornell Center for Materials Research for help with the SEM and XPS data collection. We acknowledge Ludwig Stork, Paul Müller and Claudia Klöser, RTWH Aachen University, for measurements of pXRD using Cu $K\alpha_1$ radiation and for optical absorption measurements. We acknowledge the Cornell High Energy Synchrotron Source (CHESS), supported by the NSF and NIH/NIGMS via NSF award DMR-0225180. The computational resources were performed on the Intel Cluster at the Cornell Nanoscale Facility which is a part of the National Nanotechnology Infrastructure Network (NNIN) funded by NSF. A. M. acknowledges support from Alexander von Humboldt foundation. M. L. acknowledges support from the Department of Defense (DoD) through the National Defense Science and Engineering Graduate Fellowship (NDSEG) Program. This work was supported by an NSF through Grant no. DMR-0602526.

Appendix A. Supplementary material

Supplementary material associated with this article can be found in the online version at doi:10.1016/j.jssc.2010.10.009.

Supplemental materials includes pXRD pattern of $NaTaN_2$ and of $AgTaN_2$ synthesized by using various temperatures and procedures, and a detail of determination of Ag/Ta ratio by pXRD.

References

[1] F.J. DiSalvo, S.J. Clarke, Curr. Opinion Solid State and Mater. Sci. 1 (1996) 241–249.
[2] D.H. Gregory, Coord. Chem. Rev. 215 (2001) 301–345.
[3] A. Miura, X.-D. Wen, H. Abe, G. Yau, F.J. DiSalvo, J. Solid State Chem. 183 (2010) 327–331.
[4] A. Miura, M.E. Tague, J.M. Gregoire, X.-D. Wen, R.B. van Dover, H.D. Abruña, F.J. DiSalvo, Chem. Mater. 22 (2010) 3451–3456.
[5] G.J. Snyder, A. Simon, Angew. Chem. 106 (1994) 713–715.
[6] O. Reckeweg, T.P. Braun, F.J. DiSalvo, H.-J. Meyer, Z. Anorg. Allg. Chem. 626 (2000) 62–67.
[7] P. Hohn, G. Auffermann, R. Ramlau, H. Rosner, W. Schnelle, R. Kniep, Angew. Chem. 45 (2006) 6681–6685.
[8] M.R. Fruchart, J.P. Bouchaud, M.E. Fruchart, M.G. Lorthioir, R. Madar, A. Rouault, Mater. Res. Bull. 2 (1967) 1009–1020.
[9] R.D. Shannon, D.B. Rogers, C.T. Prewitt, Inorg. Chem. 10 (1971) 713–718.
[10] U. Zachwieja, H. Jacobs, Eur. J. Solid State Inorg. Chem. 28 (1991) 1055–1062.
[11] R. Nagarajan, N. Tomar, J. Solid State Chem. 182 (2009) 1283–1290.
[12] W.C. Sheets, E.S. Stampler, M.I. Bertoni, M. Sasaki, T.J. Marks, T.O. Mason, K.R. Poeppelmeier, Inorg. Chem. 47 (2008) 2696–2705.
[13] K. Isawa, Y. Yaegashi, S. Ogota, M. Nagano, S. Sudo, K. Yamada, H. Yamauchi, Phys. Rev. B 57 (1998) 7950–7954.
[14] H. Kawazoe, M. Yasukawa, H. Hyodo, M. Kurita, H. Yanagi, H. Hosono, Nature 389 (1997) 939–942.
[15] P.F. Carcia, R.D. Shannon, P.E. Bierstedt, R.B. Flippen, J. Electrochem. Soc. 127 (1980) 1974–1978.
[16] S. Ouyang, N. Kikugawa, D. Chen, Z. Zou, J. Ye, J. Phys. Chem. C 113 (2009) 1560–1566.
[17] Y. Maruyama, H. Irie, K. Hashimoto, J. Phys. Chem. B 110 (2006) 23274–23278.
[18] H. Muguerra, C. Colin, M. Anne, M.-H. Julien, P. Strobel, J. Solid State Chem. 181 (2008) 2883–2888.
[19] S. Hashimoto, C. Tanaka, A. Murata, T. Sakurada, J. Surf. Anal. 13 (2006) 14–18.
[20] M.F. Al-Kuhaili, J. Phys. D: Appl. Phys. 40 (2007) 2847–2853.
[21] M. Bielmann, P. Schwaller, P. Ruffieux, O. Gröning, L. Schlapbach, P. Gröning, Phys. Rev. B 65 (2002) 235431.
[22] G. Kresse, J. Hafner, Phys. Rev. B 47 (1993) 558–561.
[23] G. Kresse, D. Joubert, Phys. Rev. B 59 (1999) 1758–1775.
[24] J.P. Perdew, K. Burke, M. Ernzerhof, Phys. Rev. Lett. 77 (1996) 3865–3868.
[25] A. Jacob, C. Parent, P. Boutinaud, G. Le Flem, J.P. Doumerc, A. Ammar, M. Elazhari, M. Elaatmani, Solid State Commun. 103 (1997) 529–532.
[26] H. Jacobs, E. von Pinkowski, J. Less-Common Met. 146 (1989) 147–160.
[27] W.C. Sheets, E. Mugnier, A. Barnabé, T.J. Marks, K.R. Poeppelmeier, Chem. Mater. 18 (2005) 7–20.
[28] R.D. Shannon, Acta Crystallogr. Sect. A 32 (1976) 751–767.
[29] K. Momma, F. Izumi, J. Appl. Crystallogr. 41 (2008) 653–658.